Exploration of predictors for statistical-dynamical subseasonal prediction of Western North-Pacific tropical cyclone activity in Earth system models

Hansen, Kurt A.; Janiga, Matthew A.

Publisher's version / Version de l'éditeur:

https://doi.org/10.1029/2024JD042341

Journal of Geophysical Research: Atmospheres, 130, 6, 2025-03-13

JGR Atmospheres

RESEARCH ARTICLE
10.1029/2024JD042341

Exploration of Predictors for Statistical-Dynamical Subseasonal Prediction of Western North-Pacific Tropical Cyclone Activity in Earth System Models

Kurt A. Hansen[1] and **Matthew A. Janiga**[2]

[1]National Research Council, Ottawa, ON, Canada, [2]Naval Research Lab Marine Meteorology Division, Monterey, CA, USA

Key Points:

- Tropical cyclone (TC) days appears to be the most predictable metric on subseasonal time-scales
- A signal in outgoing longwave radiation (OLR), likely tied to the Indian Ocean monsoon and independent of the Madden Julian Oscillation, is linked to Western North Pacific TC activity
- Subseasonal TC prediction in the Pacific can be improved by including a measure of this OLR signal in a statistical-dynamical model

Supporting Information:

Supporting Information may be found in the online version of this article.

Correspondence to:

K. A. Hansen,
kurt.a.hansen4.ctr@us.navy.mil

Citation:

Hansen, K. A., & Janiga, M. A. (2025). Exploration of predictors for statistical-dynamical subseasonal prediction of western north-pacific tropical cyclone activity in earth system models. *Journal of Geophysical Research: Atmospheres*, *130*, e2024JD042341. https://doi.org/10.1029/2024JD042341

Received 27 AUG 2024
Accepted 19 FEB 2025

Abstract Subseasonal prediction of tropical cyclones (TCs) has many potential applications but remains a challenge due to biases in both model-based large-scale conditions and TCs in coupled global models. Model forecasts of environmental parameters can be linked to TC activity and then be used to extend the horizon of useful skill through statistical-dynamical models. The aim of this work is to assess the utility of incorporating model forecasted environmental fields in a statistical model compared with skill coming from model forecasted Madden Julian Oscillation (MJO) state in predicting TC activity over the Western North Pacific (WNP). In this study, we evaluate the European Center for Medium-Range Weather Forecasts (ECMWF) from the Subseasonal-to-Seasonal (S2S) database and the Navy Earth System Prediction Capability (ESPC) as part of the Subseasonal Experiment on their ability to predict WNP TC activity using environmental fields. To isolate the environmental signals associated with subseasonal variability of TC activity, we examine events of anomalous accumulated cyclone energy, genesis, and TC days. These events are used to create composites of ERA5 reanalysis fields of environmental conditions related to WNP TC activity, which are used to select predictors for statistical dynamical hybrid models. The ECMWF statistical-dynamical scheme exhibits an improvement in skill by using a tailored outgoing longwave radiation (OLR) predictor compared with the MJO predictors. The Navy-ESPC generally performs worse than the ECMWF and has OLR biases that impede it from improving skill in the statistical-dynamical schemes. Using shear and humidity fields as predictors did not improve predictability in either model.

Plain Language Summary We assess skill in making forecasts of typhoons two to 4 weeks in the future, also known as the subseasonal range. Dynamical models such as the European Center for Medium-Range Weather Forecasts (ECMWF) and Navy Earth System Prediction Capability (Navy-ESPC) are generally bad at predicting typhoon activity in the subseasonal range; however, they can forecast the state of El Niño (El Niño Southern Oscillation (ENSO)) and a slow-moving pattern of thunderstorms called the Madden Julian Oscillation (MJO) which can be linked to typhoon activity. Using a dynamical model to forecast certain predictors and statistically linking those predictors to a more specific phenomenon (such as typhoons) is called a statistical-dynamical model. We found that we can improve upon forecasts of typhoon activity that use MJO and ENSO by adding another predictor that captures thunderstorm activity associated with the IO monsoon to the statistical-dynamical models. This monsoon predictor only increases skill in the ECMWF statistical-dynamical model. The IO monsoon predictor does not improve skill in the Navy-ESPC likely because of model biases.

1. Introduction

The West North Pacific (WNP) basin is the most active region for tropical cyclone (TC) activity in the world (Chan, 2005; Gray, 1979) and storms in this region regularly have devastating societal impacts (Kleinen, 2007; Q. Zhang et al., 2009, 2011). More accurate prediction of these storms is crucial in preventing loss of life and property (Q. Zhang et al., 2009; White et al., 2017). The Madden-Julian Oscillation (MJO) is the main cause of variability in TC activity on subseasonal time scales in the WNP (Liebmann et al., 1994; Xie et al., 1963) and is a significant factor in accurately predicting TC activity on these time scales (Klotzbach & Oliver, 2015; Camp et al., 2018; C.-Y. Lee et al., 2018; Zhao et al., 2022). Significant progress has been made in using dynamical coupled global models to predict TCs on subseasonal time scales (Camargo et al., 2019). Despite this progress, large biases model produced TC climatology (Gregory et al., 2020; C.-Y. Lee et al., 2018; Alano & Lee, 2016) and MJO behavior remain in most of these models (Kim et al., 2019; Rushley et al., 2022). Statistical

post-processing of these dynamical forecasts has been used to address biases in TC frequency to produce more accurate forecasts (Gregory et al., 2020; Vitart et al., 2010a). Another technique that has shown promise is relating large-scale environmental conditions from model forecasts to TC activity, also known as statistical-dynamical prediction (Hansen et al., 2022; Maier-Gerber et al., 2021; Qian et al., 2020; Vecchi et al., 2014; Zhao et al., 2022). However, there are still uncertainties regarding which parameters are useful for subseasonal prediction and how this is dependent on the biases of the individual coupled models.

One established subseasonal predictor in MJO, which is a slowly propagating global pattern of convection centered on the equator with a period of 40–90 days (Janiga et al., 2018; Jones et al., 2004; Kim et al., 2018; Madden & Julian, 1971; Xie et al., 1963). As the convectively active phase of the MJO passes through the WNP, there is an increase the number of tropical storms and typhoons (Liebmann et al., 1994). Other measures of TC activity such as accumulated cyclone energy (ACE) and major typhoons also increase when the MJO is convectively active in the West Pacific (Phases 6 and 7 of the Wheeler Hendon Index) (Klotzbach & Oliver, 2015). Several mechanisms have been proposed for how the MJO modulates WNP TC activity. Liebmann et al. (1994) and Sobel and Maloney (2000) have suggested that the MJO causes increased vorticity at 850 mb and low level convergence. Ye et al. (2020) found that the MJO is linked to increased moisture transport from the Bay of Bengal. Camargo et al. (2009) and F. Zhang et al. (2019) found that the MJO modulates WNP TC activity through changes in environmental conditions as measured by the genesis potential index (GPI). Genesis potential index is a combined measure of several environmental parameters defined by *K*. Emanuel and Nolan (2004) designed for climate prediction. Relative humidity (RH) at 600 mb appears to be the most important of the GPI components in the MJO's modulation of the TC environment (Camargo et al., 2009). Genesis potential index has proven useful on subseasonal scales; however, studies such as Hansen et al. (2020) (referred to as H20 from here on) show that GPI needs to be used cautiously on subseasonal scales as there can be large cancellations among terms.

Several other phenomena also play a role in modulating WNP TC activity, including the Southeast Asian Monsoon. Rajeevan (1993) found that annual Indian monsoon rainfall and WNP typhoon days were negatively correlated. They also found that the week of and week prior to the onset of the monsoon there is a decrease in typhoon formation. Huang and Guan (2012) found that TC activity in the South China Sea (SCS) is reduced during active monsoon years. Kumar and Krishnan (2005) hypothesized that the reduction in TC activity during active monsoon years is connected to a decrease in 850 mb vorticity over the WNP.

Another phenomenon that influences WNP TC activity is the boreal summer intraseasonal oscillation (BSISO), which is associated with north and eastward propagating convection in Southeast Asian Monsoon regions (Lawrence & Webster, 2002). You et al. (2019) found that BSISO can affect TC genesis regions in the WNP and can produce favorable atmospheric RH at 600 and 850 mb vorticity for TC genesis, although this affect is secondary to that of the MJO. Another factor may be the Mei-yu front (C.-S. Lee et al., 2006). This semi-permanent feature is a region of enhanced cloudiness and rainfall around China and Japan tied to the Southeast Asian Monsoon (Takako, 1973). The Mei-yu front often spawns low pressure systems and has been associated with individual cases of TC genesis in the SCS, although its broader impact on total WNP TC activity has not been thoroughly explored.

Additionally, the ENSO, a 3–7 years oscillation in equatorial East Pacific sea surface temperatures (SSTs) with impacts on global weather (Rasmusson & Wallace, 1983), modulates WNP TC activity. While ENSO does not tend to influence the total number of TCs in the WNP (Ramage & Hori, 1981), it does modulate typical genesis locations within the West Pacific. During the warm phase of ENSO (El Niño), enhanced TC genesis occurs further east in response to the shift in location of the monsoon trough and warmest SSTs (Lander, 1994; B. Wang & Chan, 2002). The shift in genesis location allows TCs in the WNP to last longer and become more intense during El Niño events (Camargo & Sobel, 2005; B. Wang & Chan, 2002).

Many previous studies have examined subseasonal prediction of TCs in various regions (Gregory et al., 2020; Leroy & Wheeler, 2008; Vitart et al., 2010b; Klotzbach, 2007; C.-Y. Lee et al., 2018; Camp et al., 2018; Belanger et al., 2010; Maier-Gerber et al., 2021; Zhao et al., 2022; Qian et al., 2020); however, relatively few of these focus on the WNP or use statistical-dynamical methods. Elsberry et al. (2010) looked at dynamical model European Centre for Medium-Range Weather Forecasts (ECMWF) predictions of significant TC events in the 2008 season. While the ECMWF had biases and did not correctly predict several early and late season events, there were several periods where the model appeared to have useful predictive skill on subseasonal timescales. C.-Y. Lee et al. (2018) assessed models in the Subseasonal to Seasonal (S2S) dataset on their ability to capture the MJO-TC

connection and quantified their skill in predicting TC occurrence on subseasonal timescales. They find most models are not skillful in predicting TC occurrence past 1 week, although in the WNP a few models do maintain weak but positive skill (as measured by Brier skill score [BSS]) at week two and beyond. Gregory et al. (2020) expanded on C.-Y. Lee et al. (2018) and found that predictions of ACE have similar skill to TC occurrence and genesis is the most difficult aspect of TCs to forecast on subseasonal timescales.

Previous studies have used statistical-dynamical hybrid models to produce skillful forecasts (H. Wang et al., 2009). This traditionally involves taking the output of dynamical models, from which a few key predictors are calculated, and feeding these values into a statistical model that outputs a forecast probability for an event. Qian et al. (2020) used a statistical-dynamical approach, taking a variety of parameters, such as OLR (a proxy for convection) and vertical shear, from Geophysical Fluid Dynamics Laboratory forecasts and used them to forecast 10 day TC occurrence in the WNP. They found that this hybrid approach produced skillful forecasts out to 5 weeks whereas the individual statistical and dynamical forecasts generally had no skill after 10 days (using temporal correlation coefficient and receiver operating characteristic area under curve) demonstrating the incredible potential for statistical-dynamical methods in the subseasonal timeframe. Zhao et al. (2022) created and analyzed a statistical-dynamical model based on the ECMWF forecasts of TCs, ENSO state, and OLR which was used to create MJO and Quasi Bi-weekly oscillation predictors. They were used to forecast weekly TC genesis in three sub-basins in the WNP. Skill of the statistical-dynamical scheme that used all predictors (using Brier skill) performed better than climatology out to 5 weeks.

Statistical-dynamical methods can improve subseasonal TC prediction in the WNP and other basins. However, there are still many open questions, such as: What are the most skillful predictors for subseasonal TC predictions and what measures of TC activity are easiest to predict? In this study, we utilize the compositing method from H20 to determine environmental conditions associated with WNP TC activity that can be used as predictive variables. We then evaluate the ECMWF and Navy Earth System Prediction Capability (Navy-ESPC) forecasts to assess the skill provided by different predictors and for different measures of TC activity in a statistical-dynamical framework. We find TC days (the total duration of all TCs in a 7-day period) to be the most predictable measure of TC activity and the MJO the largest contributor to subseasonal predictability. Although environmental fields such as shear and humidity did not increase skill in a statistical-dynamical framework, we find another potential source of predictability, IO convection, that may be associated with the Southeast Asian Monsoon, though only the ECMWF sees skill increase with this new predictor. In Sections 2 and 3, we discuss the data and methods. In Section 4, we go over the environmental signals associated with subseasonal WNP TC activity, and in Section 5, we discuss predictability of these signals in models. We provide remarks in Section 6.

2. Data

2.1. TC Data

Six-hourly TC data from the Joint Typhoon Warning Center best track database are retrieved from the International Best Track Archive for Climate Stewardship (Knapp et al., 2010, IBTrACS). Tropical cyclone activity is quantified using genesis, TC days, and ACE, defined as the summation of the square of the maximum sustained surface winds (in knots) for a TC at each six-hour interval (Bell et al., 2000). For this study, all TC metrics are calculated for storms in the WNP south of 30°N during the June through November (JJASON) period. Values of ACE, TC days, and genesis put through 7 day running means from which anomalies are computed with respect to a 50 day running mean of the seasonal cycle of TC activity based on 1979–2020 climatology. This is done to smooth over weather scales and remove the seasonal cycle, although this still captures inter-seasonal variability.

2.2. Reanalysis Data

Thermodynamic and dynamic fields are calculated or taken directly from the ERA5 database (Hersbach et al., 2020). Hourly data are available at 137 vertical levels on a 0.25° grid, although for this study only 0000 UTC data at four vertical levels and 1.25° horizontal resolution are used for faster computation. Sea surface temperature data are used in calculating the values of ENSO regions, the IO Dipole (IOD), and WNP SST anomalies.

2.3. Dynamical Models

The Navy-ESPC is a fully coupled Earth system model with atmosphere, land, ocean, and ice components (Barton et al., 2021). The spectral resolution of the atmospheric model in Navy ESPC is about 37 km with 60 vertical levels which is sufficient for the generation of TCs (Moon et al., 2018). For the years 1999–2015, 45 day reforecasts were initialized four times a week for the Subseasonal Experiment (SubZ, Pegion et al., 2019) yielding 1485 forecasts. For the period of 2009–2015, atmospheric initial conditions were taken from a consistent analysis dataset generated using the Navy-ESPC while prior years were initialized using operational Navy Operational Global Atmospheric Prediction System analyses. For this study, we only considered the first 30 days of the deterministic forecasts and only forecasts initialized during June through October to ensure that verification occurs during JJASON. Reforecast data provided values of 500 mb RH, zonal and meridional winds at 850 and 200 mb used to calculate vertical wind shear, and OLR was used to calculate the two principal components (PCs) of the real-time OLR MJO index (ROMI) (Kiladis et al., 2014) (see section 3a). Navy Earth System Prediction Capability forecasted anomalies were calculated relative to the model climatology of forecasts initialized within the same month from years 1999–2015.

The European Center for Medium-range Weather Forecasting (ECMWF) is a fully coupled Earth system model with atmosphere, land, ocean, and ice components (Vitart, 2014). There is a grid interval of about 55 km and 50 vertical levels. 46 day reforecasts as part of the S2S project (Vitart et al., 2017) were made twice a week for the years 2001–2020 yielding 860 forecasts. As with the Navy-ESPC only the first 30 day of the deterministic forecasts are considered and only forecasts initialized in June-October are included. As with the Navy-ESPC, forecasted anomalies are calculated relative to ECMWF forecasts initialized during the same month from years 2001–2020.

For comparison of Navy-ESPC and ECMWF skill in Figures 12 and 13, only forecasts of years in both datasets (2001–2015) were considered to ensure consistency, though, results are similar if the full datasets are used.

The Navy-ESPC and ECMWF models are able to skillfully predict the MJO to lead times of 20 days and thus give us confidence that they will be useful for subseasonal TC prediction (Kim et al., 2019; S. Wang et al., 2019). However, we expect the ECMWF to have better performance as has higher and longer lasting MJO forecast skill. Janiga et al. (2018) demonstrated that the Navy-ESPC overstates MJO convective activity (which is unique among SubX and S2S models Kim et al. (2019)). Rushley et al. (2022) attributed the positive MJO amplitude bias to exaggerated vertical moisture advection, whereas the positive MJO propagation bias east of the Maritime Continent (MC, the land mass between IO and Pacific) was due to latent heat flux biases.

3. Methods

3.1. Predictors

Several predictors are created using the persistence of SSTs; the Niño 3.4 region (5°S−5°N, 120–170°W), Niño four region (5°S−5°N, 160°E−150°W), the IOD ([10°S−10°N 50°E–70°E] - [10°S−0°S 90°E–110°E]), and WNP SST anomalies (7.5°N–22.5°N, 110°W–160°W). Indices are calculated using a 90 day trailing running mean of SSTs in the defined regions.

For both reforecast and reanalysis, the MJO is measured using ROMI which uses the empirical orthogonal functions (EOFs) found by Kiladis et al. (2014) which were used to calculate the MJO PCs. A benefit of using ROMI is that it also captures the northward propagation of convection associated with BSISO (S. Wang et al., 2018). The first two PCs of ROMI are used as predictors for the statistical-dynamical model. When calculating the OLR anomalies in the model forecasts and in the reanalysis fields, we remove the 50 day running mean climatology based on 1979–2020 ERA5 data to obtain OLR anomalies. We then remove the 40 day running mean of OLR to remove the ENSO signal. Forecasts are padded with reanalysis data for 20 days prior to the initialization date, and both the forecasts and verification are padded with zeros following the 45 day forecast period when calculating the values of the PCs. From the PCs the MJO can be classified as one of eight phases or in a neutral/inactive state if the MJO is below the 1.0 magnitude threshold.

Several environmental fields were also considered for predictors. Gray (1979) identified several environmental parameters that influence the development of TCs, particularly humidity, vertical wind shear, ocean temperature, and vorticity. These are each assessed individually for their influence on WNP TC activity, and based on their climatological relation to subseasonal TC activity were tested as predictors in the statistical dynamical models.

K. Emanuel and Nolan (2004) created an index that subjectively condensed all these environmental conditions into a single value called the GPI. Genesis potential index was shown to correlate well with TC genesis on climatological timescales. Genesis potential index is defined as:

$$GPI = |10^5\eta|^{3/2}\left(\frac{RH}{50}\right)^3\left(\frac{PI}{70}\right)^3(1+0.1V_{Shear})^{-2} \quad (1)$$

where η is 850 mb vorticity, RH is 700 mb RH in percent, potential intensity (PI) is PI in m s^{-1} which is the maximum theoretical intensity of a hurricane considering the SST and atmospheric profile defined in K. A. Emanuel (1987), and V_{Shear} is the 200–850 mb vertical wind shear magnitude in m s^{-1}.

3.2. Determining Environmental Predictors

To find subseasonal patterns in environmental fields that indicate enhanced subseasonal TC activity we use variants of the compositing method ACE by Year (ABY) from H20. ACE by Year was shown to highlight patterns associated with the MJO and other subseasonal factors while removing signals from ENSO. The selection of periods that go into an ABY composite is done by taking the top 33% of normalized pentad ACE anomaly events from each year. The running mean of ACE smooths out weather signals, and the normalized anomaly removes the seasonal cycle. The selection of an equal number of periods from each year ensures that oscillations that impact TC activity on seasonal scales, such as ENSO, are averaged out. In this study, we use a 7 day running mean as opposed to the original 5 days from H20 to be consistent with the weekly forecast scheme that is more common for operational use. We also use variants of ABY based on TC days and genesis instead of ACE to make a TC days By Year (TCDBY) composite, and Genesis by Year (GBY) composite. Composites of shear, winds at various levels, RH, PI, GPI, SST, vorticity, and OLR are taken producing an environmental pattern that is associated with simultaneous subseasonally active TC periods as defined by ABY, TCDBY, and GBY composites. These ABY, TCDBY, and GBY composites are used to create predictors based on area-average anomalies over regions with highest anomalies or using a spatial correlation coefficient of the forecasted field with the reanalysis TCDBY composite. As in H20, reanalysis composites remove environmental conditions within 500 km radius of a TC center, although we have also analyzed the composites with no removal of TCs and with a 1000 km radius removal around TCs.

3.3. Statistical Models

To create probabilistic forecasts, we use multiple logistic regression models. The logistic models have the form:

$$P = \frac{1}{1+e^{\beta_0+\beta_1x_1+\beta_2x_2+\cdots+\beta_nx_n}} \quad (2)$$

Where P is the probability of an event occurring, $(x_1, x_2,\ldots,x_n)$ are the values of the predictors with n representing the number of predictors and $(\beta_0,\beta_1,\ldots,\beta_n)$ being the coefficients determined from the training data. The logistic regression model is trained using a predictor dataset built from persistence SST values and Navy-ESPC or ECMWF reforecasts of OLR, the PCs of the MJO, and various measures of environmental conditions such as vertical wind shear and winds at different levels. Different predictive schemes are made by training the logistic model on a subset of the parameters in the predictor dataset, the parameters used in each scheme will be identified in the figures and text. Logistic forecasts are verified against the binary value of above average or below average weekly TC activity relative to the 50 day running mean of the seasonal cycle unless otherwise noted. We assess TC days, ACE, and genesis from IBTrACS as the verification metrics for TC activity. Training data for the logistic model exclude data from the year of the forecast to avoid over-fitting of the model. The logistic model is run using the statsmodel Python module and uses the liblinear solver.

3.4. Verification Metrics

To evaluate the model skill of probabilistic forecasts we primarily use the BSS (Wilks, 2011) which compares the mean error of probabilistic forecasts to those of a reference or climatological forecast. Brier skill score values greater than zero indicate skillful forecasts. Brier skill score is based on the Brier score (BS), defined as:

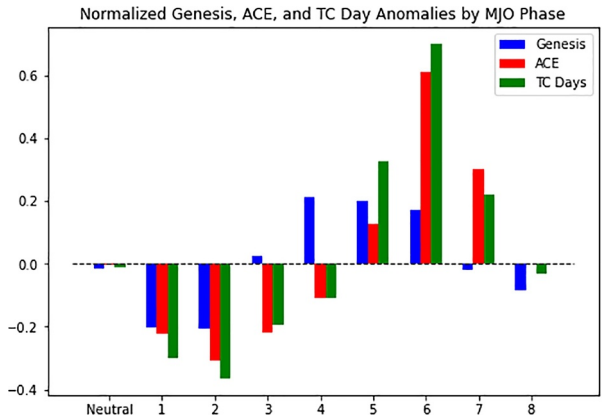

Figure 1. Anomalies in accumulated cyclone energy, tropical cyclone (TC) Genesis, and TC days within the Western North Pacific Basin (0°N–30°N, 100°E–180°E) associated with each Madden Julian Oscillation phase.

$$BS = \frac{1}{N}\sum_{t=1}^{N}(f_t - o_t)^2 \tag{3}$$

where N is the number of forecasts, f_t is the individual forecast probability of an event and o_t is the observed outcome (zero or one) of events. Brier skill score is defined as:

$$BSS = 1 - \frac{BS}{BS_{Ref}} \tag{4}$$

where BS is the skill of the model and BS_{Ref} is the reference skill. In this study, BS_{Ref} is based on a constant forecast of the JJASON climatological odds of experiencing an above average period for TC activity (roughly 0.4) (Because TCs are rare events, there is a nonnormal distribution of TC activity and the odds of any given period being above average is less than 50%). It is worth reiterating that skill in this study is measured using TC anomalies relative to the seasonal cycle which is a high standard. Other studies frequently use seasonal mean climatology as BS_{Ref} which may complicate direct comparisons of skill values across studies. Statistical testing uses a two-tailed two-sample student's *t* test and is evaluated at the 95% level.

4. Environmental Signals

Figure 1 shows the average value of various TC metrics in the WNP in association with each MJO phase. Anomalies of each metric are calculated with respect to the 50 day smoothed seasonal cycle, then these anomalies themselves are put through a 7 day running mean. To normalize the values of the TC metrics,the seasonal cycle of the daily standard deviation of each metric is calculated then put through a 50 day running mean. The smoothed anomalies are then divided by the smoothed seasonal cycle standard deviation to get the normalized anomalies. This is shown in Equation 5 with subscripts indicating running mean over *n* days.

$$ACE'_7(day, year) = \frac{(ACE_1(day, year) - ACE_{50,climo}(day))_7}{ACE_{50,sdev}(day)} \tag{5}$$

In the WNP, most TC activity occurs in MJO Phase 6, but this is dependent on the method of defining TC activity. Tropical cyclone genesis actually occurs well prior to MJO Phase 6 with Phases 4, 5, and 6 having about the same peak amplitude. A peak in TC days occurs slightly earlier than peak ACE although both have the strongest response in MJO Phase 6. From this chart, it is clear that TC genesis is not as strongly connected to the MJO as ACE or TC days as the maximum amplitude in normalized genesis anomalies peaks at about 0.2. Accumulated cyclone energy and TC days have a much stronger signal in association with the MJO with peak normalized anomalies near 0.6. Tropical cyclone days appear to have a slightly higher magnitude of normalized anomalies in both the most active and least active phases of the MJO. This suggests that for subseasonal predictions, forecasts of TC days should provide the best predictability as it has the strongest ties with the predominant source of predictability, the MJO.

The location of ACE, TC days, and genesis events occurring during subseasonally active periods is shown in Figure 2. Most TC activity occurs in the open WNP to the north east of the Philippines. Genesis primarily occurs at slightly lower latitudes, between 10°N and 20°N. Three distinct maxima are seen in the genesis regions, one in the SCS, one immediately to the east of the Philippines, and one further east between 140°E and 150°E. Accumulated cyclone energy and TC days tend to have peak activity at slightly higher latitude, centered around 20°N, and are more concentrated around 130°E in longitude. This is most likely because of prevailing steering patterns that take TCs from genesis regions to the northwest (with reduced frequency over land) (Camp et al., 2019; B. Wang et al., 2013).

Figure 3a shows normalized GPI anomalies during periods of anomalously high genesis. While the compositing method is still the same as described in Section 3.2, the rarity of genesis events makes the GBY composite

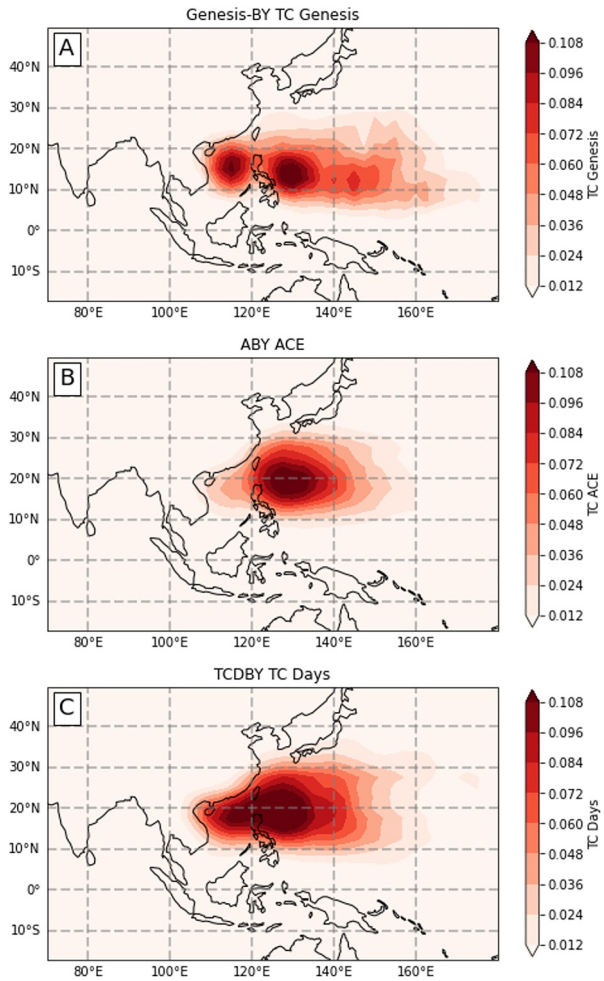

Figure 2. Composites of average rates of (a) genesis, (b) accumulated cyclone energy, and (c) tropical cyclone (TC) days occurring within 500 km of a given point during subseasonally active TC periods as measured by their respective subseasonal compositing technique (Genesis by Year, TC days By Year, and ACE by Year) (see Section 3b for description of these techniques).

essentially a composite of 7 day periods centered on genesis events. This composite shows broadly positive GPI anomalies over the WNP in development regions. Given that incipient disturbances just prior to genesis were not removed, some of this signal may be more representative of mesoscale systems than the incipient environment. However, GPI has much weaker anomalies in association with other measures of TC activity. The GPI anomaly in TCDBY composites (Figure 3c) over the WNP between 10°N and 20°N are still positive but not statistically significant. There is a region of below average GPI south of regions with the most TC activity that has significant negative GPI anomalies. The composite based on ACE shows a similar pattern. Thus basin-average or sub-basin-scale-average GPI may be a complicated and unhelpful predictor of TC activity. Given GPI is well correlated with seasonal variability of TC activity and is a combination of several environmental parameters with well-established connections to TC activity on weather scales, we might have expected a stronger signal. However, our findings are similar to H20 which found little correlation of weekly GPI with Atlantic TC activity. The WNP does have significant above average GPI during subseasonally active TC periods but only if TCs are not removed from the composite (Figure S1 in Supporting Information S1). This suggests that positive GPI anomalies during active subseasonal periods are primarily just a measure of TCs themselves and not the ambient environment. We will look at the individual components of GPI as there may be stronger competing signals that counteract each other to produce a weak GPI signal.

As GBY, ABY, and TCDBY produce similar composite fields, we will only show TCDBY composites from here on due to the strong connection of TC Days to the MJO and the use of TCDBY composites in the statistical-dynamical predictions. In Figure 4a, 850–200 mb vertical wind shear anomalies in the TCDBY composite are higher than average over the WNP basin during periods of subseasonally active TC activity. These seem to be primarily responsible for the negative GPI anomalies just south of regions with the most TC activity. This is a somewhat counter-intuitive result as high vertical wind shear is generally considered unfavorable for TC activity. However, this result is not wholly unsurprising; H20 found high wind shear anomalies over portions of the tropical Atlantic in association with active subseasonal periods in that basin.

If we break down the components of the shear into upper level and lower level components we can gain more insight into the physical processes that are occurring during these active periods and the signal of higher than average shear becomes more logical. In Figure 4b we see an inflow channel into the WNP basin coming from the IO at mid and lower levels (the plot shows 500 mb winds and RH as humidity at this level is especially influential on TCs, although 850 mb winds and humidity have similar patterns). This flow pattern may provide a series of favorable conditions (moisture transport, vorticity, lower level convergence). At upper levels (Figure 4c) winds are divergent over TC areas which is also evidenced by negative 200 mb velocity potential anomalies seen over much of the WNP. There are two apparent upper level outflow channels; one flowing from the WNP to the northwest across China, and another that broadly arcs north across Japan before turning east, then south, then southwest while increasing in velocity and crossing Indonesia and flowing into the southern IO. Dual upper level outflow channels are associated with strong TCs in the WNP (Lin et al., 2024). Environmental conditions within 500 km of TC centers were removed suggesting these inflow and outflow features are not a direct measure of the TCs themselves. These features are still apparent after removal of environmental conditions within 1,000 km of TC centers (Figure S2 in Supporting Information S1). However, it is still certainly possible that these signals in lower level and upper level winds are only capturing the broader circulation of TCs as opposed to the ambient environment. Shear anomalies appear to be strongly connected to the MJO as the favorable MJO Phase 6 has a very similar wind structure in this region.

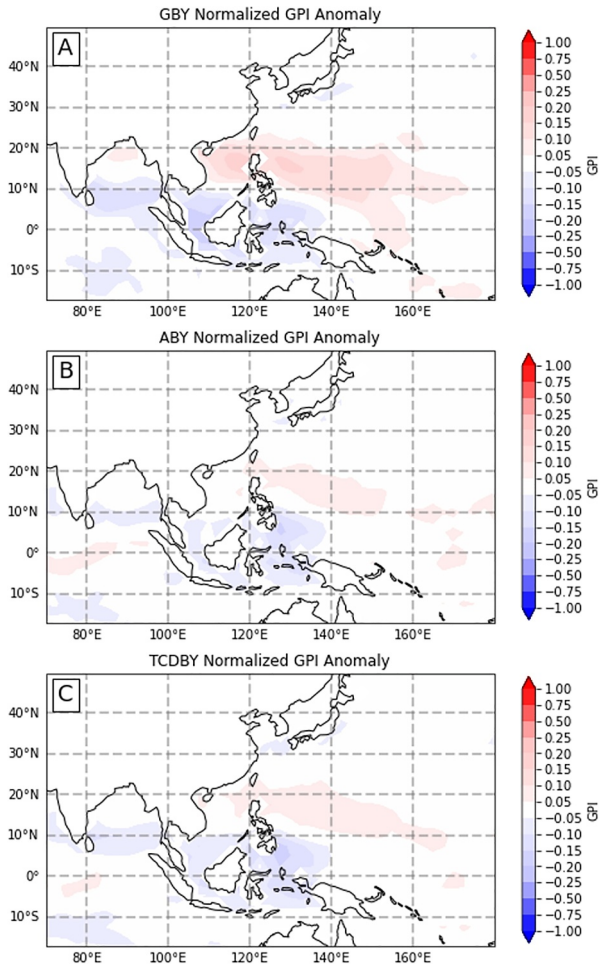

Figure 3. Normalized genesis potential index anomalies associated with the top third of subseasonal tropical cyclone (TC) events as measured by (a) Genesis, (b) accumulated cyclone energy, and (c) TC days.

Relative humidity (Figure 5) has notable anomalies, although the signal is not as strong as for shear. Drier anomalies exist around the MC, consistent with MJO Phases 6 and 7. Positive RH biases exist over portions of the WNP basin. Increased moisture could certainly contribute to both genesis and the intensification/persistence of TCs. The RH anomaly pattern appears very similar to that of the favorable MJO Phase 6 which is in agreement with Ye et al. (2020).

850 mb vorticity anomalies are above average in TCDBY composites if TCs are included, but are much closer to neutral when TCs are removed. As seen in Figure 6, there is a region of positive vorticity anomalies in the SCS and to a lesser extent the eastern Philippine Sea which are favored regions for TC genesis, and this may be a signal that environmental vorticity plays a role in subseasonal TC activity. The GBY composites (Figure S3 in Supporting Information S1) have a stronger vorticity signal and show a statistically significant area of positive vorticity anomalies in the SCS. The vorticity anomalies also point to low-level inflow from the IO in agreement with Figure 4b.

Potential intensity (Figure S4 in Supporting Information S1) appears to be generally lower than average during active TC periods. The reduction of PI appears dependent on SSTs which are also below average in TCDBY composites. Reduced PI may just be a signal of upwelling caused by the TCs or increased cloud cover.

The breakdown of GPI suggests that increased RH and vorticity may play a small role in creating a favorable environment for subseasonal TC activity. The PI signal is hard to disentangle from the TCs themselves but may counteract the positive influences of RH and vorticity. The strongest signal appears tied to geographically specific dynamic patterns, specifically inflow and outflow channels as evidenced by the robust shear anomalies in the TCDBY composite. The composites of wind and RH are similar to those found for MJO Phase 5 and 6 from previous studies (Hao et al., 2020). Genesis potential index and many of its components only have weak anomalies in association with subseasonal TC activity. Components with strong anomalies, primarily shear and RH, appear tied to the MJO suggesting that these environmental fields may not be useful as independent predictors. We next look at OLR patterns to assess features that influence subseasonal TC variability.

In Figure 7, there are negative OLR anomalies over the WNP and positive OLR anomalies over the North IO and the MC associated with active TC periods. The negative OLR anomalies over the WNP suggest that enhanced convection occurs in this region during active TC periods. Other than the shear signal, this region of negative OLR anomalies has the highest magnitude normalized anomalies we have seen in the subseasonal composites. As the 500 km environment surroundings TCs is removed, this signal is not likely associated with the TCs themselves.

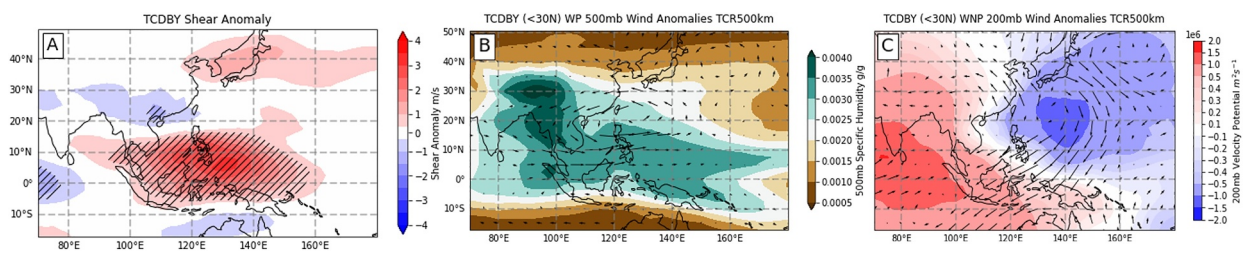

Figure 4. (a) Normalized 200–850 mb vertical wind shear anomalies associated with the top third of subseasonal tropical cyclone (TC) events as measured by TC days. Anomalies that are significant at the 95% level are hatched. Genesis, and accumulated cyclone energy, (b) 500 mb level wind anomalies (vectors) and 500 mb level specific humidity anomalies (shaded), and (c) 200 mb level wind anomalies (vectors) and 200 mb level divergence anomalies.

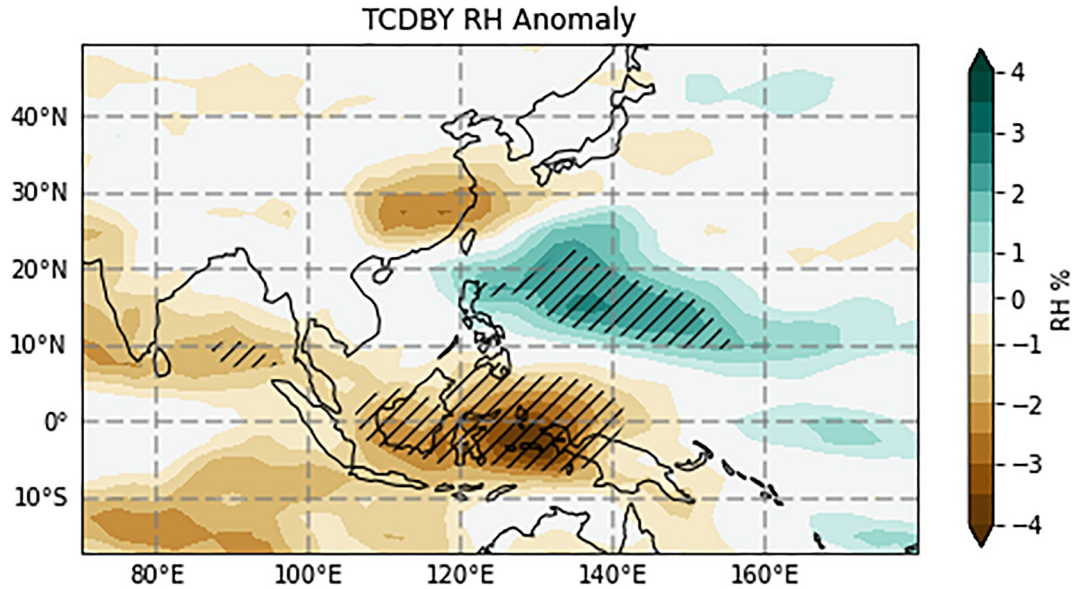

Figure 5. Relative humidity anomalies associated with the top third of subseasonal tropical cyclone (TC) events as measured by TC days. Anomalies that are significant at the 95% level are hatched.

These features are still clearly identifiable even using a 1,000 km radius of removal around TCs (Figure S5 in Supporting Information S1). This suggests that there is increased convective activity not associated with TCs themselves, but rather in association with incipient disturbances or as a result of a more favorable large-scale environment, which spurs TC activity.

As seen in Figures 8a and 8b, the positive OLR anomalies match well with the OLR anomalies associated with the favorable phase of the MJO (Phase 6) which is also characterized by decreased convection over the North IO and MC. While the TCDBY OLR composite (Figure 8b) clearly shows the influence of the MJO on WNP TC activity, there are some key distinctions between the two composites.

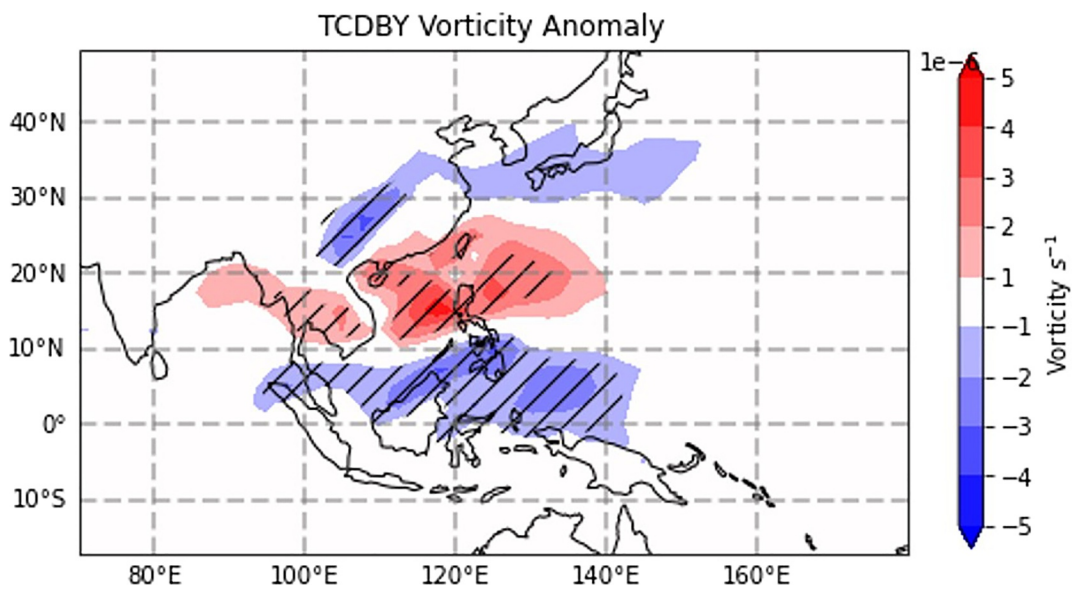

Figure 6. Normalized vorticity anomalies associated with the top third of subseasonal tropical cyclone (TC) events as measured by TC days. Anomalies that are significant at the 95% level are hatched.

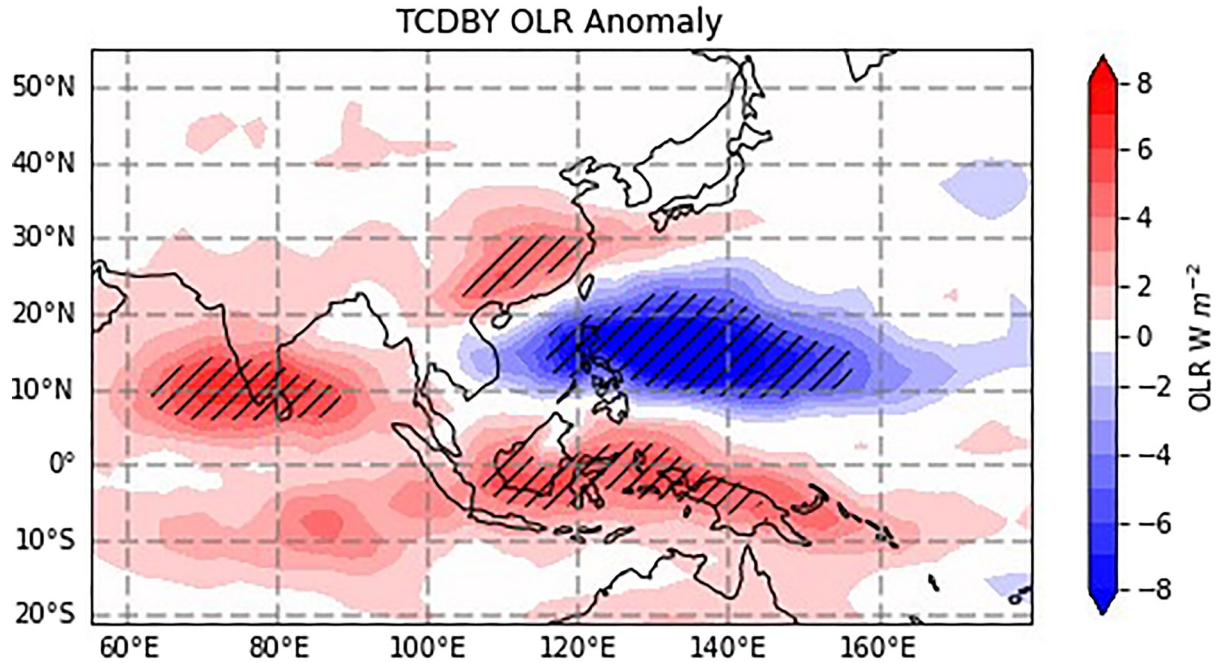

Figure 7. Normalized outgoing longwave radiation anomalies associated with the top third of subseasonal tropical cyclone (TC) events as measured by TC days. Anomalies that are significant at the 95% level are hatched.

The region with the highest discrepancy appears to be around the Bay of Bengal (Figure 8c). While the negative OLR anomalies over the WNP are roughly the same magnitude for both the MJO and TCDBY composites, the positive OLR anomalies over the Bay of Bengal and surrounding regions in the IO and MC are much weaker in the TCDBY composite. The geographic location of these differences in anomalies implicates the Indian Monsoon as another potential factor that may influence WNP TC activity. Several previous studies have implicated the Indian monsoon as a factor determining WNP TC activity, Kumar and Krishnan (2005) and Huang and Guan (2012) found that there is a negative correlation between seasonal typhoon and TC activity in the WNP in association with various measures of the Indian monsoon. The negative OLR anomalies in Figure 8c also align with the OLR anomalies seen during inactive monsoon regimes as in Turner and Hannachi (2010). The inactive monsoon regimes from Turner and Hannachi (2010) also exhibit low level flow regimes similar to our Figure 4b. There are other regions with discrepancies in OLR between the MJO and TCDBY composites. Positive OLR anomalies over coastal China may indicate a weakening of the Mei-Yu front. Positive OLR anomalies in the Central Pacific may indicate a relatively rapid (subseasonal scale) cooling of SSTs in ENSO regions leading to an increase in WNP TC activity on subseasonal scales. However, these signals appear comparatively weak and these connections are speculative.

Because we are using ROMI, we should capture the more northerly summertime patterns of the MJO/BSISO and thus these discrepancies in the TCDBY composite are likely not artifacts of the seasonal cycle or BSISO. The TCDBY composite by design is meant to capture the superposition of all potential signals influencing subseasonal

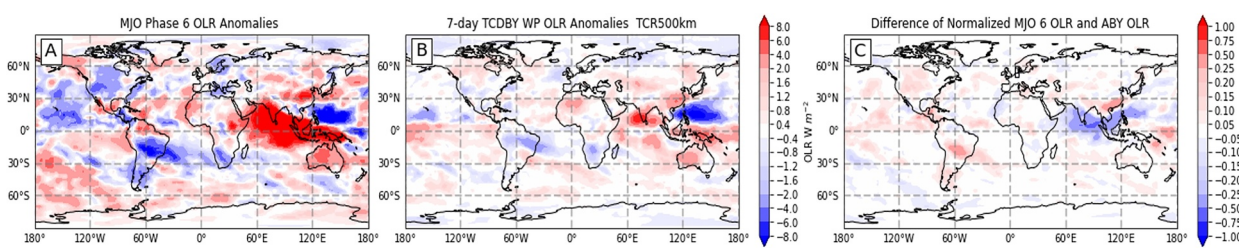

Figure 8. Composites of outgoing longwave radiation anomalies in ERA5 reanalysis data during (a) Madden Julian Oscillation Phase 6, (b) TC days By Year periods, and Panel (c) shows the difference between (a) and (b) normalized by their respective highest amplitude anomalies.

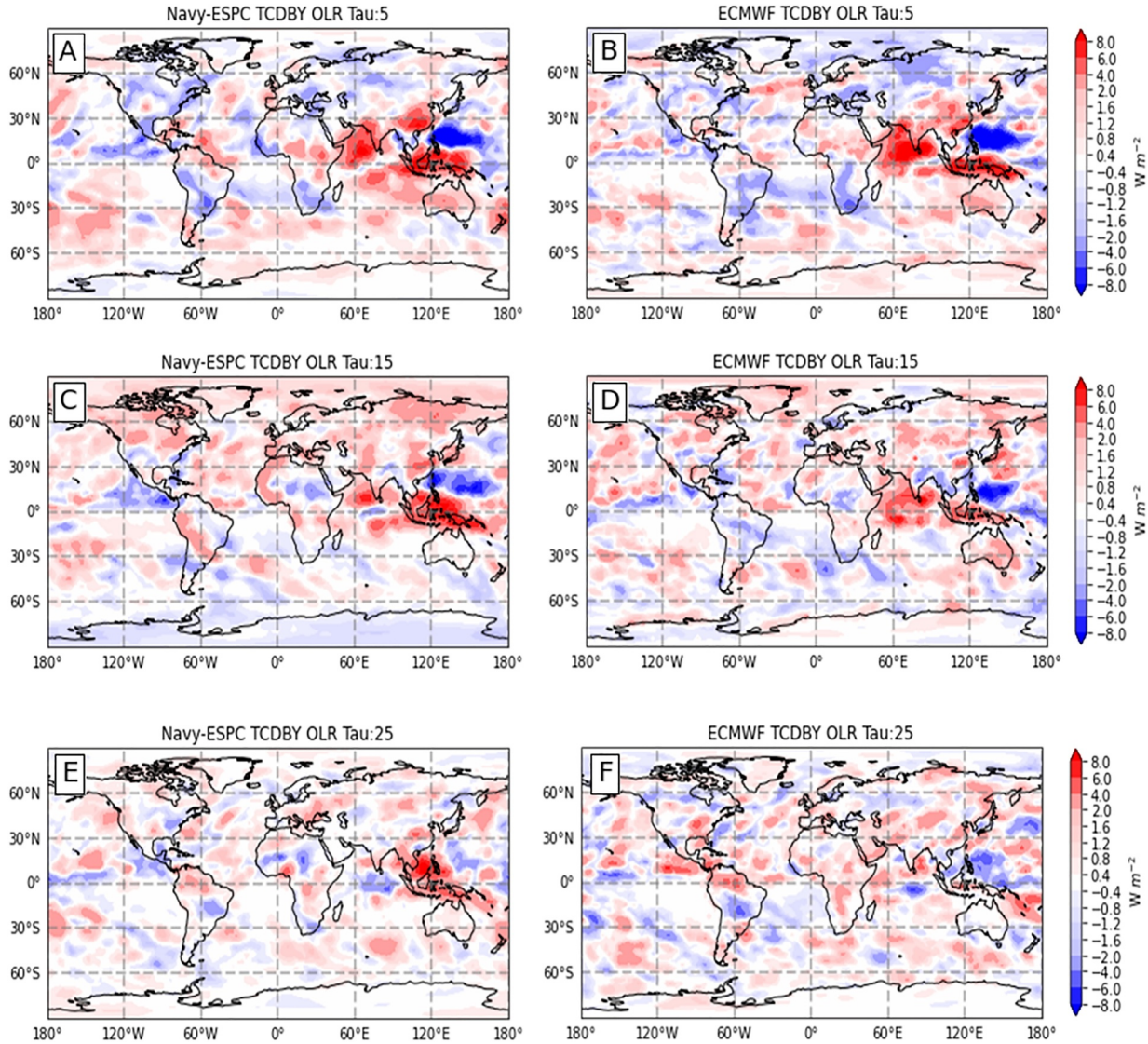

Figure 9. Composites of forecasted outgoing longwave radiation during TC days By Year periods (as determined by observed tropical cyclone data) as produced by (a), (c), (e) the Navy Earth System Prediction Capability, and (b), (d), (f) European Center for Medium-Range Weather Forecasts models at forecast lead times of (a), (b) 5 days, (c), (d) 15 days, and (e), (f) 25 days.

variability of WNP TC activity. We cannot easily pull apart the signals shown in the composite. However, we can test if these signals provide additional predictability by comparing the TCDBY metrics to the MJO PCs in a statistical-dynamical model.

While the EOFs of the MJO are most commonly used for subseasonal predictions, both for WNP TCs and more broadly, the TCDBY composites suggest that other physical features influence subseasonal variability of WNP TCs that may provide additional predictability. However, these features may not be captured well by models or may be inherently less predictable. To assess the potential utility of these OLR patterns, we assess the ability of the ECMWF and Navy-ESPC models to capture the subseasonal OLR signals as a function of lead time.

5. Modeling Results

Next, we evaluate the ability of the Navy-ESPC and the ECMWF to recreate the subseasonal OLR signal. As seen in Figures 9a and 9b initially and for short lead times (up to 5 days), both the Navy-ESPC and ECMWF models reproduce the subseasonal OLR signal and even appear to capture distinctive features such as the weaker OLR

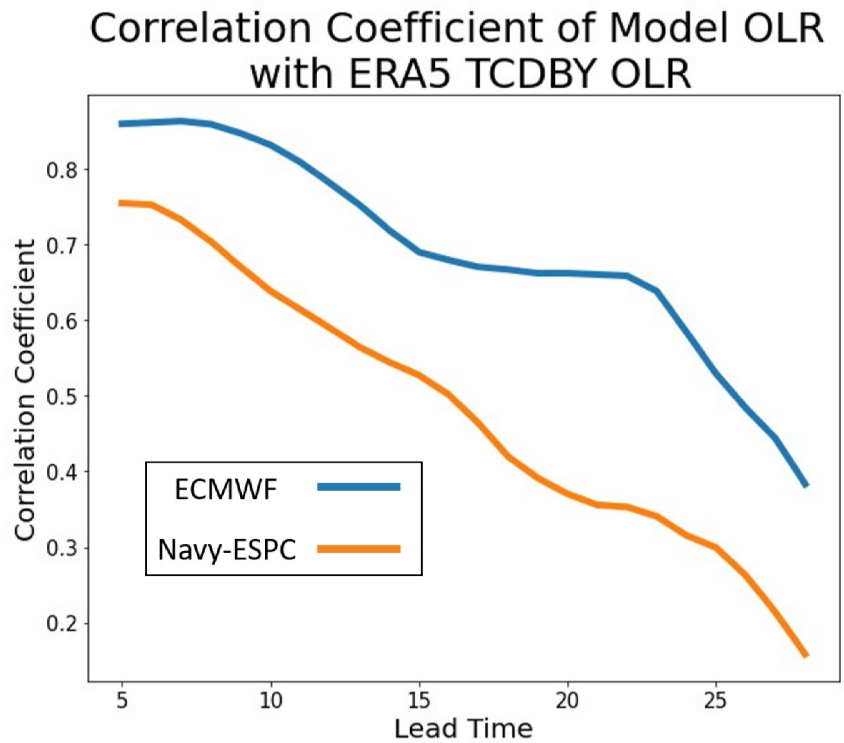

Figure 10. The spatial correlation between the ERA5 reanalysis TC days By Year (TCDBY) composite of 7 day running mean outgoing longwave radiation (OLR) and the TCDBY composite of Navy Earth System Prediction Capability and European Center for Medium-Range Weather Forecasts forecasted OLR as a function of lead time.

anomalies over equatorial IO. For forecasts of OLR anomalies, verifying during TCDBY periods with 15 day lead times, the signals are still generally accurate. Both models capture higher OLR over India and the MC and lower OLR over the WNP. Discrepancies and significant errors become apparent at day 25. The ECMWF is still able to capture the signals of anomalously low OLR over the WNP and higher OLR over India and eastern MC; however, these anomalies are much weaker. However, the ECMWF at least maintains the OLR pattern in the IO, while the Navy-ESPC OLR pattern is greatly degraded. Notably, in Figure 9e, positive OLR anomalies exist over the WNP and there is a large region of negative OLR anomalies near southern India which is nearly opposite the reanalysis TCDBY composite. This suggests that the Navy-ESPC is misrepresenting physical mechanisms that are important for WNP TC activity. The Navy-ESPC errors may be related to the fast phase-speed bias of the MJO in that model (Rushley et al., 2022).

We quantify the models ability to reproduce TCDBY signals using a spatial correlation coefficient (Figure 10) between the forecasted OLR anomalies in the ECMWF and Navy-ESPC models that verified during TCDBY periods and the reanalysis TCDBY composite in the global region between 30°S and 30°N. The ECMWF outperforms the Navy-ESPC at all lead times. The discrepancy between the ECMWF and Navy-ESPC appears to peak between days 20 and 25 which is in the critical subseasonal range. These results reflect the ability of these models to forecast ROMI. S. Wang et al. (2019) showed that the ECMWF produces skillful forecasts of ROMI to about 30 days during boreal summer using ranked probability skill score, which is also what Kim et al. (2019) found using correlation coefficient. Kim et al. (2019) also showed that the Navy-ESPC performed worse than the ECMWF, with the correlation coefficient dropping below the skillful threshold (0.5) at 20 days. We see similar discrepancies in skill in Figure 10 with the ECMWF correlation coefficient dropping below 0.5 10 days after the Navy-ESPC. However, both models lose about 5 days of skill when predicting the TCDBY OLR metric, suggesting another less predictable phenomenon potentially degrades skill (see Table 1).

Next, we assess statistical-dynamical hybrid models, both for the immediately useful results of finding the most skillful model and predictive scheme, but also to determine what physical features are contributing to the predictability and at what lead times.

Table 1
Explanation of Predictors in Statistical-Dynamical Schemes

Predictor	Description
MJO	Two predictors: dynamical model forecasts of the first two principal components of the MJO
Nino4	Persistence forecast of 3 month average SST anomalies in the Niño4 region
SST Suite	Four predictors: Persistence forecast of SST anomalies representing Niño4, Niño3.4, the Indian Ocean Dipole, and WNP ocean
ABY RH	The anomaly correlation coefficient of dynamical model forecasted 700 mb RH anomalies with reanalysis ABY composite of RH anomalies
ABY Shear	Same as ABY RH but for dynamical model forecasts of 200–850 mb vertical wind shear
ABY OLR	Same as ABY RH but for dynamical model forecasts of OLR

The statistical-dynamical schemes were built with a handful of predictors and always include persistence forecasts of SSTs in the Niño 4 region (though other ocean parameters were tested; explained further down) as well as dynamical model forecasts of either MJO PCs, or the correlation coefficient of forecasted OLR anomalies with the reanalysis TCDBY OLR composite. Other fields were also tested, such as various measures of vertical wind shear magnitude or RH. A list and explanation of predictors can be found in Table. 1. The statistical-dynamical schemes are trained to predict above or below average weekly TC days, and result in a probabilistic forecast that was used to calculate BSS. The models are trained on all reforecast data except those from the year of the forecast to ensure independence of results.

To assess the statistical significance of the skill of the statistical-dynamical models, training data were randomly resampled to create a random variant of the statistical-dynamical model and used to produce a new forecast. This was repeated to generate a suite of statistical dynamical forecast "ensembles." For the ECMWF, 860 ensembles were generated and 1485 ensembles were used for the Navy-ESPC, matching the number of reforecasts available from each model. Regardless of the model, lead-time, or scheme, the BSS produced by the suite had a fairly regular distribution, with the BSS falling within ±0.01 of the average value 95% of the time.

We will now look at the utility of various predictors in the statistical-dynamical schemes. Figure 11 shows the BSS of various predictive schemes in predicting active TC periods using the Navy-ESPC. We found that the Niño

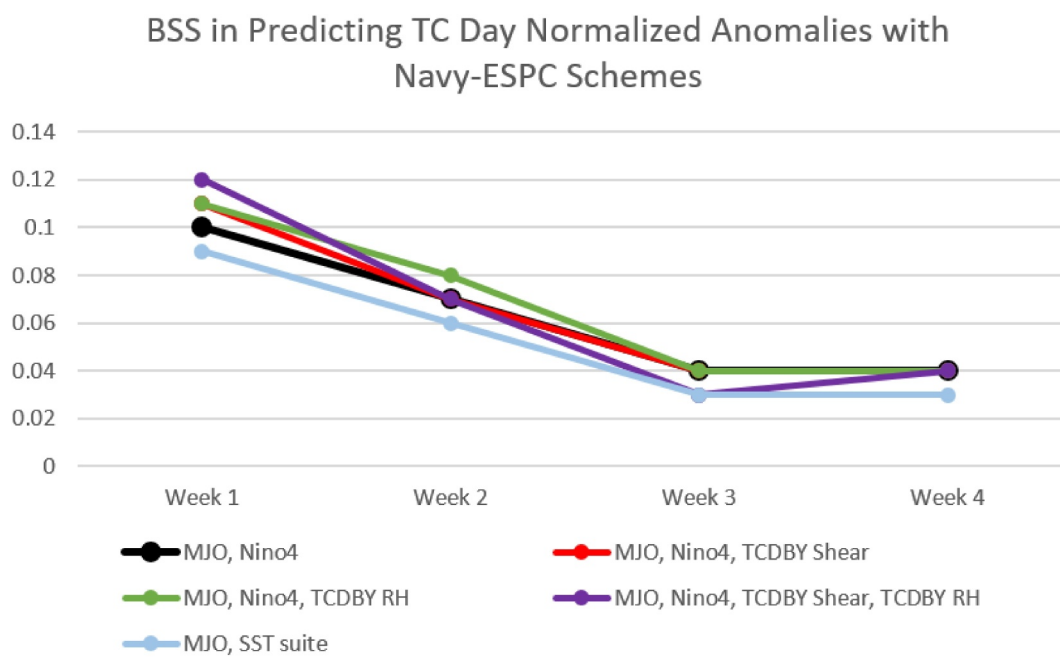

Figure 11. The Brier skill score of various statistical-dynamical schemes using the Navy Earth System Prediction Capability (1999–2015). Predictors included in each scheme are shown in the key below the plot. Further explanation of predictors can be found in Table 1.

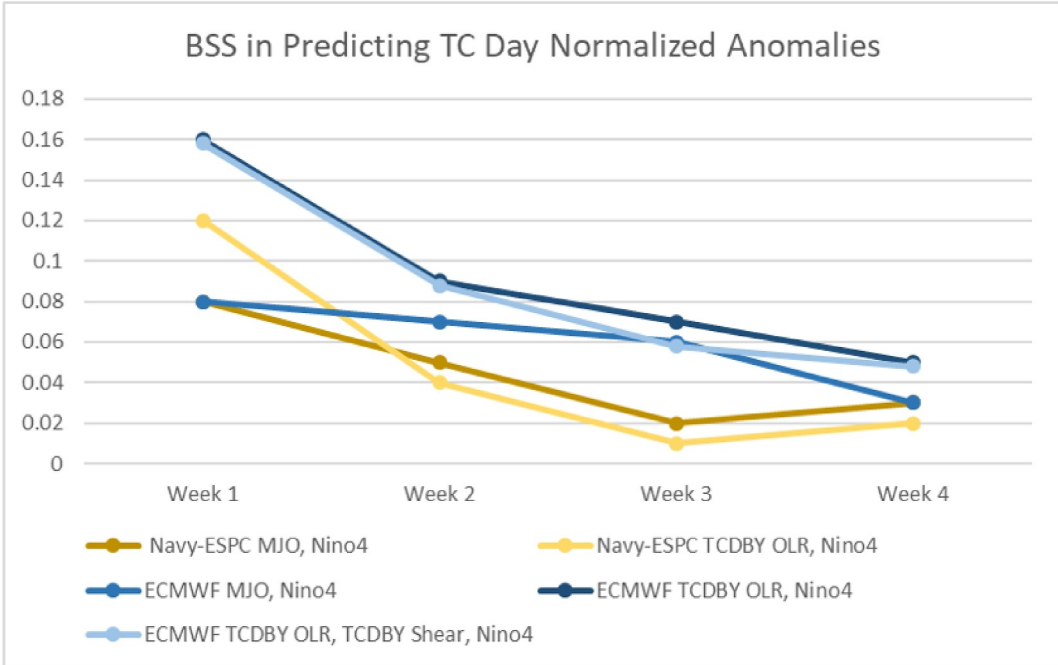

Figure 12. The Brier skill score of various predictive schemes using the Navy Earth System Prediction Capability and European Center for Medium-Range Weather Forecasts (2001–2015). Predictors included in each scheme are shown in the key below the plot. Further explanation of predictors can be found in Table 1.

4 region resulted in the highest contribution of skill of the four SST predictors that we tested. Including the complete suite of SST predictors (IO, WNP, Niño 3.4, and Niño 4 region) resulted in little change or a slight decrease in skill. It is best practice to use independent predictors in logistic regression models, thus all future analysis will only include Niño 4 as an SST predictor.

We have assessed the utility of several environmental predictors in the Navy-ESPC model, particularly vertical wind shear and RH as these had the strongest anomalies in association with subseasonal TC activity. In Figure 11, forecasted values of RH and shear are quantified using correlation coefficient with their respective reanalysis TCDBY composite using correlation coefficient and used as a predictor in the statistical-dynamical scheme. Neither predictor results in a significant improvement of skill at any lead time compared with the scheme that only uses the MJO and Niño 4 predictors. Using both RH and shear as predictors does result in a higher BSS during week 1; however, skill is slightly reduced at all subsequent lead times and thus do not appear useful in the subseasonal timeframe. Other variants of shear predictors were tested including a tropics only correlation coefficient (globally between 10°S and 10°N), and regionally averaged shear anomalies based on significant regions in the TCDBY composite such as the WNP (0°N–20°N 112.5°E–162.5°E) and west IO (15°S−14°N 50°E–80°E). None of these predictors resulted in an increase in skill. Variants of RH predictors that were tested include forecasted RH anomalies averaged over the WNP (10°N–20°N 112.5°E–162.5°E for RH) and correlation coefficients of the forecasted RH field with reanalysis ABY and GBY composites. These variants also did not result in a significant increase in skill at any lead time.

Although the use of environmental fields as predictors in the statistical-dynamical framework results in a consistent lack of improvement to skill, OLR has a stronger connection to subseasonal TC activity and has varied ties to different physical mechanisms which have yielded more fruitful results.

As suggested by Figures 10 and 12, it is confirmed that the Navy-ESPC has lower skill than the ECMWF in predicting TC activity. For equivalent predictive schemes, the Navy-ESPC has a lower BSS than the ECMWF at all lead times. The highest discrepancy appears to be around week 3.

One particularly crucial finding is that the ECMWF scheme, that incorporates correlation coefficients of OLR TCDBY composites, performs better at all lead times than the scheme that uses MJO PCs. This implies that some

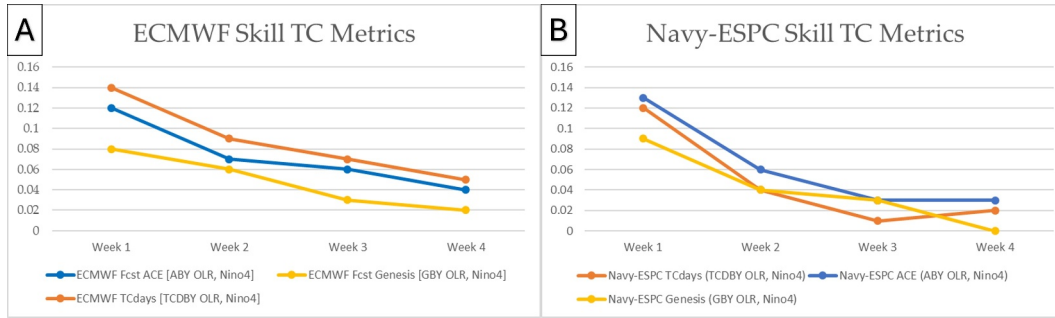

Figure 13. The Brier skill score of the outgoing longwave radiation and Niño predictive schemes in predicting various measures of tropical cyclone activity using (a) the European Center for Medium-Range Weather Forecasts, and (b) the Navy Earth System Prediction Capability. The key shows the dynamical model used followed by the predicted variable. Predictors for each scheme are identified in the key in parentheses. Further explanation of predictors can be found in Table 1.

feature in the OLR field that is not represented by the MJO aids in prediction of TCs in the WNP. The Navy-ESPC, does not see an improvement in skill by incorporating OLR TCDBY forecasts in the subseasonal timeframe suggesting it is only drawing predictability from the MJO and SSTs. This suggests misrepresentation of OLR patterns in the Asian Monsoon region may be hurting the Navy-ESPCs performance. This is also supported by the discrepancy in BSS as a function of lead time between the ECMWFand Navy-ESPC which peaks around 3 weeks. This is similar to the discrepancy between the correlation coefficient of the TCDBY OLR patterns in these two models from Figure 10 which also peaks at 3 weeks. The mirroring of OLR correlation coefficients and BSS suggests that a failure in representing the spatial pattern of OLR particularly in the Indian monsoon region is limiting the Navy-ESPC's skill. The ECMWF also performs better than the Navy-ESPC, especially at week three when using the MJO PCs as predictors, suggesting that the established MJO propagation bias in the Navy-ESPC also hampers skill.

For completeness, we also show the ECMWF scheme that incorporates correlation coefficient of predicted shear with the TCDBY shear composite. Including this shear predictor had no impact in skill or even caused a slight decrease in skill in the ECMWF. We found that the upper and lower wind fields in the ABY composite closely match that of MJO Phase 6. Thus shear is likely not providing any additional predictability when added to a scheme that already accounted for by the MJO. While many of the environmental predictors have been disappointing, it is worth emphasizing that the TC specific OLR pattern did result in an increase in skill in the ECMWF demonstrating there is more skill to be gleaned from the subseasonal timeframe.

As suggested by Figure 1, BSS for predicting TC days was higher than BSS for ACE or TC genesis using the ECMWF as seen in Figure 13a. The BSS for predicting above average ACE periods is nearly as skillful as TC days in the ECMWF. Genesis predictions, however, appear to be much more difficult and have worse skill. A peak in genesis events does usually lead a peak in ACE or TC days by about 5 days, but even extending the genesis skill out 5 days does not result in more skillful forecasts than the unaltered TC days forecast scheme. The Navy-ESPC has generally worse skill for all metrics and also does not show as clear of a distinction between skill in forecasting different TC metrics in the statistical-dynamical paradigm.

6. Conclusion

Our most pertinent result is that we find a pattern of OLR that can be used as a predictor to improve subseasonal TC forecasts. The OLR pattern associated with enhanced WNP TC activity has similarities with the OLR pattern for MJO Phase 6. However, there are clear distinctions between the TCDBY composite and MJO composite. Primarily, there are weaker positive OLR anomalies over the Bay of Bengal and adjacent regions indicating enhanced convection, at least compared with MJO Phase 6. The discrepancy in OLR pattern is similar to the OLR pattern produced during inactive Southeast Asian Monsoon periods. The Southeast Indian monsoon may provide a source of predictability for subseasonal variability of WNP TCactivity, which is supported by Kumar and Krishnan (2005) and Huang and Guan (2012). The TCDBY composite also has anomalously high OLR over coastal China. This points to an environmental phenomenon, perhaps the Mei-Yu front or Southeast Asian Monsoon that may provide a source of predictability for subseasonal TC prediction.

The ECMWF is able to capture the subseasonal OLR signal better than the Navy-ESPC. As a result, the ECMWF sees an increase in BSS by 0.01–0.02 (around a 20% increase in skill) when forecasting anomalous TC days in the subseasonal timeframe when incorporating this OLR pattern. Using the TCDBY technique to composite forecasted conditions in association with observed TC activity, we find the ECMWF appears to not only capture the MJO pattern but also the anomalously weak OLR anomalies in the IO. The Navy-ESPC does initially capture these features, however loses the secondary OLR signal around two weeks lead time and does not even appear to resolve the MJO around week three. The largest discrepancy between the models ability to recreate the TCDBY OLR signal appears to at lead times of 21–28 days, which coincides with the greatest discrepancy in the statistical-dynamical skill of the models.

We also tested various environmental fields as potential predictors of TC activity. We have found that there is increased vertical wind shear over the WNP during periods of increased TC activity. In fact, this shear signal is the strongest environmental signal we have found in connection to subseasonal TC activity. These wind patterns appear to be strongly tied to the MJO and using these fields as predictors in a statistical-dynamical model to forecast TC activity does not result in an additional improvement in skill over using the MJO PCs. Relative humidity also did not prove to be a useful predictor and other components of GPI had weak anomalies in association with subseasonal TC activity.

In a basin-integrated sense, TC days appears to be the most predictable metric for TC activity on subseasonal scales at least using the ECMWF, the most skillful model (using BSS and spatial correlation coefficient). This result was expected given the stronger relation between the MJO and TC days when compared with genesis. However, environmental conditions such as the components of GPI and OLR appear to be more strongly tied to genesis than either TC days or ACE. These results would suggest that the statistical dynamical approach we have used would be more skillful at predicting genesis. There is no clear reason for this discrepancy. Perhaps genesis being a relatively rare and single event makes it difficult to predict statistically.

The statistical-dynamical models provide skillful forecasts through week four regardless of the scheme or base dynamical model. However, the ECMWF outperforms the Navy-ESPC for all schemes and lead times. These results are based on the single-members and we expect skill would be improved by incorporating the ensemble suite. The ECMWF, as part of a statistical-dynamical hybrid model, sees an increase in skill when incorporating the spatial OLR pattern as compared with using the MJO PCs. The Navy-ESPC sees a slight decrease in skill when incorporating the spatial OLR pattern. We attribute these differences to the ability of the model to recreate the TCDBY pattern, the ECMWF having better representation of OLR appears to be rewarded with an increase in skill. This is also an important finding as it suggests that a feature that is not associated with the MJO is providing a source of predictability that can be utilized. Further research is needed to establish the physical mechanisms that contribute to the TCDBY pattern and how it influences WNP TC activity. This study has already implicated the Southeast Asian Monsoon and that we suggest that more research can be conducted tying this feature to WNP TC activity and determining the predictability of this feature.

Data Availability Statement

Madden Julian Oscillation EOF data are available from (Kiladis et al., 2014). The IBTrACS dataset that was used to calculate TC metrics can be found at (Knapp et al., 2010). The ERA5 dataset used to calcualte ABY and shear composites can be found at (Hersbach et al., 2020). The SubX dataset can be found at (Pegion et al., 2019). European Center for Medium-Range Weather Forecasts reforecasts can be found at (Vitart, 2014).

Acknowledgments
We gratefully acknowledge the support of the Chief of Naval Research through the NRL Base Program, Extended-Range TC Prediction 6.2 (PE 62435N). Computational resources were supported in part by a grant of HPC time and resources from the Department of Defense High Performance Computing Modernization Program, Stennis Space Center, MS.

References

Alano, E., & Lee, M. (2016). Natural disaster shocks and macroeconomic growth in asia: Evidence for typhoons and droughts. *Asian Development Bank Economics Working Paper Series*, *503*. Retrieved from https://doi.org/10.2139/ssrn.2894778

Barton, N., Metzger, E. J., Reynolds, C. A., Ruston, B., Rowley, C., Smedstad, O. M., et al. (2021). The navy's earth system prediction capability: A new global coupled atmosphere-ocean-sea ice prediction system designed for daily to subseasonal forecasting. *Earth and Space Science*, *8*(4), e2020EA001199. Retrieved from https://doi.org/10.1029/2020EA001199

Belanger, J. I., Curry, J. A., & Webster, P. J. (2010). Predictability of North Atlantic tropical cyclone activity on intraseasonal time scales. *Monthly Weather Review*, *138*(12), 4362–4374. https://doi.org/10.1175/2010MWR3460.1

Bell, G. D., Halpert, M. S., Schnell, R. C., Higgins, R. W., Lawrimore, J., Kousky, V. E., et al. (2000). Climate assessment for 1999. *Bulletin of the American Meteorological Society*, *81*(6), S1–S50. https://doi.org/10.1175/1520-0477(2000)81[s1:CAF]2.0.CO;2

Camargo, S. J., Camp, J., Elsberry, R. L., Gregory, P. A., Klotzbach, P. J., Schreck, C. J., et al. (2019). Tropical cyclone prediction on subseasonal time-scales. *Tropical Cyclone Research and Review*, *8*(3), 150–165. (Special Issue for the 9th WMO International Workshop on Tropical Cyclones) Retrieved from https://doi.org/10.1016/j.tcrr.2019.10.004

Camargo, S. J., & Sobel, A. H. (2005). Western north pacific tropical cyclone intensity and enso. *Journal of Climate*, *18*(15), 2996–3006. Retrieved from https://doi.org/10.1175/JCLI3457.1

Camargo, S. J., Wheeler, M. C., & Sobel, A. H. (2009). Diagnosis of the MJO modulation of tropical cyclogenesis using an empirical index. *Journal of the Atmospheric Sciences*, *66*(10), 3061–3074. https://doi.org/10.1175/2009JAS3101.1

Camp, J., Roberts, M. J., Comer, R. E., Wu, P., MacLachlan, C., Bett, P. E., et al. (2019). The western pacific subtropical high and tropical cyclone landfall: Seasonal forecasts using the met office glosea5 system. *Quarterly Journal of the Royal Meteorological Society*, *145*(718), 105–116. Retrieved from https://doi.org/10.1002/qj.3407

Camp, J., Wheeler, M. C., Hendon, H. H., Gregory, P. A., Marshall, A. G., Tory, K. J., et al. (2018). Skilful multiweek tropical cyclone prediction in ACCESS-S1 and the role of the MJO. *Quarterly Journal of the Royal Meteorological Society*, *144*(714), 1337–1351. https://doi.org/10.1002/qj.3260

Chan, J. (2005). Interannual and interdecadal variations of tropical cyclone activity over the western north pacific. *Meteorology and Atmospheric Physics*, *89*(1–4), 143–152. https://doi.org/10.1007/s00703-005-0126-y

Elsberry, R. L., Jordan, M. S., & Vitart, F. (2010). Predictability of tropical cyclone events on intraseasonal timescales with the ECMWF monthly forecast model. *Asia-Pacific Journal of Atmospheric Sciences*, *46*(2), 135–153. https://doi.org/10.1007/s13143-010-0013-4

Emanuel, K., & Nolan, D. (2004). Tropical cyclone activity and the global climate system. In *26th conference on hurricanes and tropical meteorology* (pp. 240–241).

Emanuel, K. A. (1987). The dependence of hurricane intensity on climate. *Nature*, *326*(6112), 483–485. Retrieved from https://doi.org/10.1038/326483a0

Gray, W. M. (1979). Hurricanes: Their formation, structure and likely role in the tropical circulation. meteorology over the tropical oceans. *Royal Meteorological Society*, 155–218.

Gregory, P., Vitart, F., Rivett, R., Brown, A., & Kuleshov, Y. (2020). Subseasonal forecasts of tropical cyclones in the southern hemisphere using a dynamical multimodel ensemble. *Weather and Forecasting*, *35*(5), 1817–1829. Retrieved from https://doi.org/10.1175/WAF-D-20-0050.1

Hansen, K. A., Majumdar, S. J., & Kirtman, B. P. (2020). Identifying subseasonal variability relevant to atlantic tropical cyclone activity. *Weather and Forecasting*, *35*(5), 2001–2024. Retrieved from https://doi.org/10.1175/WAF-D-19-0260.1

Hansen, K. A., Majumdar, S. J., Kirtman, B. P., & Janiga, M. A. (2022). Testing vertical wind shear and nonlinear mjo–enso interactions as predictors for subseasonal atlantic tropical cyclone forecasts. *Weather and Forecasting*, *37*(2), 267–281. Retrieved from https://doi.org/10.1175/WAF-D-21-0107.1

Hao, L., He, L., Ma, N., Liang, S., & Xie, J. (2020). Relationship between summer precipitation in north China and madden–julian oscillation during the boreal summer of 2018. *Frontiers in Earth Science*, *8*. https://doi.org/10.3389/feart.2020.00269

Hersbach, H., Bell, B., Berrisford, P., Hirahara, S., Horányi, A., Muñoz-Sabater, J., et al. (2020). The era5 global reanalysis. *Quarterly Journal of the Royal Meteorological Society*, *146*(730), 1999–2049. Retrieved from https://doi.org/10.1002/qj.3803

Huang, Q., & Guan, Y. (2012). Does the asian monsoon modulate tropical cyclone activity over the south China sea? *Chinese Journal of Oceanology and Limnology*, *30*(6), 960–965. Retrieved from https://doi.org/10.1007/s00343-012-1273-x

Janiga, M. A., Schreck, C. J., Ridout, J. A., Flatau, M., Barton, N. P., Metzger, E. J., & Reynolds, C. A. (2018). Subseasonal forecasts of convectively coupled equatorial waves and the MJO: Activity and predictive skill. *Monthly Weather Review*, *146*(8), 2337–2360. https://doi.org/10.1175/MWR-D-17-0261.1

Jones, C., Waliser, D. E., Lau, K. M., & Stern, W. (2004). Global occurrences of extreme precipitation and the madden–julian oscillation: Observations and predictability. *Journal of Climate*, *17*(23), 4575–4589. https://doi.org/10.1175/3238.1

Kiladis, G. N., Dias, J., Straub, K. H., Wheeler, M. C., Tulich, S. N., Kikuchi, K., et al. (2014). A comparison of olr and circulation-based indices for tracking the mjo. *Monthly Weather Review*, *142*(5), 1697–1715. Retrieved from https://doi.org/10.1175/MWR-D-13-00301.1

Kim, H., Janiga, M. A., & Pegion, K. (2019). Mjo propagation processes and mean biases in the subx and s2s reforecasts. *Journal of Geophysical Research: Atmospheres*, *124*(16), 9314–9331. Retrieved from https://doi.org/10.1029/2019JD031139

Kim, H., Vitart, F., & Waliser, D. E. (2018). Prediction of the madden–julian oscillation: A review. *Journal of Climate*, *31*(23), 9425–9443. Retrieved from https://doi.org/10.1175/JCLI-D-18-0210.1

Kleinen, J. (2007). Historical perspectives on typhoons and tropical storms in the natural and socio-economic system of nam dinh (vietnam). *Journal of Asian Earth Sciences*, *29*(4), 523–531. Retrieved from (Morphodynamics of the Red River Delta, Vietnam) https://doi.org/10.1016/j.jseaes.2006.05.012

Klotzbach, P. J. (2007). Revised prediction of seasonal Atlantic basin tropical cyclone activity from 1 august. *Weather and Forecasting*, *22*(5), 937–949. https://doi.org/10.1175/WAF1045.1

Klotzbach, P. J., & Oliver, E. C. J. (2015). Variations in global tropical cyclone activity and the madden-julian oscillation since the midtwentieth century. *Geophysical Research Letters*, *42*(10), 4199–4207. https://doi.org/10.1002/2015GL063966

Knapp, K. R., Kruk, M. C., Levinson, D. H., Diamond, H. J., & Neumann, C. J. (2010). The international best track archive for climate stewardship (ibtracs). *Bulletin of the American Meteorological Society*, *91*(3), 363–376. Retrieved from https://doi.org/10.1175/2009BAMS2755.1

Kumar, V., & Krishnan, R. (2005). On the association between the indian summer monsoon and the tropical cyclone activity over northwest pacific. *Current Science*, *88*(4), 602–612. Retrieved 2023-04-06, from http://www.jstor.org/stable/24110260

Lander, M. A. (1994). An exploratory analysis of the relationship between tropical storm formation in the western north pacific and enso. *Monthly Weather Review*, *122*(4), 636–651. Retrieved from https://doi.org/10.1175/1520-0493(1994)122⟨0636:AEAOTR⟩2.0.CO;2

Lawrence, D. M., & Webster, P. J. (2002). The boreal summer intraseasonal oscillation: Relationship between northward and eastward movement of convection. *Journal of the Atmospheric Sciences*, *59*(9), 1593–1606. Retrieved from https://doi.org/10.1175/1520-0469(2002)059⟨1593:TBSIOR⟩2.0.CO;2

Lee, C.-S., Lin, Y.-L., & Cheung, K. K. W. (2006). Tropical cyclone formations in the south China sea associated with the mei-yu front. *Monthly Weather Review*, *134*(10), 2670–2687. Retrieved from https://doi.org/10.1175/MWR3221.1

Lee, C.-Y., Camargo, S. J., Vitart, F., Sobel, A. H., & Tippett, M. K. (2018). Subseasonal tropical cyclone genesis prediction and MJO in the S2S dataset. *Weather and Forecasting*, *33*(4), 967–988. https://doi.org/10.1175/WAF-D-17-0165.1

Leroy, A., & Wheeler, M. C. (2008). Statistical prediction of weekly tropical cyclone activity in the Southern Hemisphere. *Monthly Weather Review*, *136*(10), 3637–3654. https://doi.org/10.1175/2008MWR2426.1

Liebmann, B., Hendon, H. H., & Glick, J. D. (1994). The relationship between tropical cyclones of the western pacific and indian oceans and the madden-julian oscillation. *Journal of the Meteorological Society of Japan. Ser. II*, *72*(3), 401–412. https://doi.org/10.2151/jmsj1965.72.3_401

Lin, Y., Chu, K., & Tan, Z.-M. (2024). Characteristics of tropical cyclone outflow over the western north pacific. *Atmospheric and Oceanic Science Letters*, 100479. Retrieved from https://doi.org/10.1016/j.aosl.2024.100479

Madden, R. A., & Julian, P. R. (1971). Detection of a 40–50 day oscillation in the zonal wind in the tropical Pacific. *Journal of the Atmospheric Sciences*, *28*(5), 702–708. https://doi.org/10.1175/1520-0469(1971)028⟨0702:DOADOI⟩2.0.CO;2

Maier-Gerber, M., Fink, A. H., Riemer, M., Schoemer, E., Fischer, C., & Schulz, B. (2021). Statistical–dynamical forecasting of subseasonal north atlantic tropical cyclone occurrence. *Weather and Forecasting*, *36*(6), 2127–2142. Retrieved from https://doi.org/10.1175/WAF-D-21-0020.1

Moon, J.-Y., Wang, B., Lee, S.-S., & Ha, K.-J. (2018). An intraseasonal genesis potential index for tropical cyclones during northern hemisphere summer. *Journal of Climate*, *31*(22), 9055–9071. Retrieved from https://doi.org/10.1175/JCLI-D-18-0515.1

Pegion, K., Kirtman, B. P., Becker, E., Collins, D. C., LaJoie, E., Burgman, R., et al. (2019). The subseasonal experiment (subx): A multimodel subseasonal prediction experiment. *Bulletin of the American Meteorological Society*, *100*(10), 2043–2060. Retrieved from https://doi.org/10.1175/BAMS-D-18-0270.1

Qian, Y., Hsu, P.-C., Murakami, H., Xiang, B., & You, L. (2020). A hybrid dynamical-statistical model for advancing subseasonal tropical cyclone prediction over the western north pacific. *Geophysical Research Letters*, *47*(20), e2020GL090095. Retrieved from https://doi.org/10.1029/2020GL090095

Rajeevan, M. (1993). Interrelationship between nw pacific typhoon activity and indian summer monsoon on inter-annual and intra-seasonal time-scale. *Mausam*, *44*(1), 109–111. https://doi.org/10.54302/mausam.v44i1.4974

Ramage, C. S., & Hori, A. M. (1981). Meteorological aspects of el nino. *Monthly Weather Review*, *109*(9), 1827–1835. Retrieved from https://doi.org/10.1175/1520-0493(1981)109⟨1827:MAOEN⟩2.0.CO;2

Rasmusson, E. M., & Wallace, J. M. (1983). Meteorological aspects of the el nino/southern oscillation. *Science*, *222*(4629), 1195–1202. Retrieved from https://doi.org/10.1126/science.222.4629.1195

Rushley, S. S., Janiga, M. A., Ridout, J. A., & Reynolds, C. A. (2022). The impact of mean-state moisture biases on mjo skill in the navy espc. *Monthly Weather Review*, *150*(7), 1725–1745. Retrieved from https://doi.org/10.1175/MWR-D-21-0225.1

Sobel, A. H., & Maloney, E. D. (2000). Effect of enso and the mjo on western north pacific tropical cyclones. *Geophysical Research Letters*, *27*(12), 1739–1742. Retrieved from https://doi.org/10.1029/1999GL011043

Takako, A. (1973). Large scale aspects of the characteristic features of the baiu front. *Papers in Meteorology and Geophysics*, *24*(2), 157–188. https://doi.org/10.2467/mripapers1950.24.2_157

Turner, A. G., & Hannachi, A. (2010). Is there regime behavior in monsoon convection in the late 20th century? *Geophysical Research Letters*, *37*(16). Retrieved from https://doi.org/10.1029/2010GL044159

Vecchi, G. A., Delworth, T., Gudgel, R., Kapnick, S., Rosati, A., Wittenberg, A. T., et al. (2014). On the seasonal forecasting of regional tropical cyclone activity. *Journal of Climate*, *27*(21), 7994–8016. Retrieved from https://doi.org/10.1175/JCLI-D-14-00158.1

Vitart, F. (2014). Evolution of ecmwf sub-seasonal forecast skill scores. *Quarterly Journal of the Royal Meteorological Society*, *140*(683), 1889–1899. Retrieved from https://doi.org/10.1002/qj.2256

Vitart, F., Ardilouze, C., Bonet, A., Brookshaw, A., Chen, M., Codorean, C., et al. (2017). The subseasonal to seasonal (s2s) prediction project database. *Bulletin of the American Meteorological Society*, *98*(1), 163–173. Retrieved from https://doi.org/10.1175/BAMS-D-16-0017.1

Vitart, F., Leroy, A., & Wheeler, M. C. (2010a). A comparison of dynamical and statistical predictions of weekly tropical cyclone activity in the southern hemisphere. *Monthly Weather Review*, *138*(9), 3671–3682. Retrieved from https://doi.org/10.1175/2010MWR3343.1

Vitart, F., Leroy, A., & Wheeler, M. C. (2010b). A comparison of dynamical and statistical predictions of weekly tropical cyclone activity in the Southern Hemisphere. *Monthly Weather Review*, *138*(9), 3671–3682. https://doi.org/10.1175/2010MWR3343.1

Wang, B., & Chan, J. C. L. (2002). How strong enso events affect tropical storm activity over the western north pacific. *Journal of Climate*, *15*(13), 1643–1658. Retrieved from https://doi.org/10.1175/1520-0442(2002)015⟨1643:HSEEAT⟩2.0.CO;2

Wang, B., Xiang, B., & Lee, J.-Y. (2013). Subtropical high predictability establishes a promising way for monsoon and tropical storm predictions. *Proceedings of the National Academy of Sciences*, *110*(8), 2718–2722. Retrieved from https://doi.org/10.1073/pnas.1214626110

Wang, H., Schemm, J.-K. E., Kumar, A., Wang, W., Long, L., Chelliah, M., et al. (2009). A statistical forecast model for atlantic seasonal hurricane activity based on the ncep dynamical seasonal forecast. *Journal of Climate*, *22*(17), 4481–4500. Retrieved from https://doi.org/10.1175/2009JCLI2753.1

Wang, S., Ma, D., Sobel, A. H., & Tippett, M. K. (2018). Propagation characteristics of bsiso indices. *Geophysical Research Letters*, *45*(18), 9934–9943. Retrieved from https://doi.org/10.1029/2018GL078321

Wang, S., Sobel, A. H., Tippett, M. K., & Vitart, F. (2019). Prediction and predictability of tropical intraseasonal convection: Seasonal dependence and the maritime continent prediction barrier. *Climate Dynamics*, *52*(9–10), 6015–6031. Retrieved from https://doi.org/10.1007/s00382-018-4492-9

White, C. J., Carlsen, H., Robertson, A. W., Klein, R. J., Lazo, J. K., Kumar, A., et al. (2017). Potential applications of subseasonal-to-seasonal (s2s) predictions. *Meteorological Applications*, *24*(3), 315–325. Retrieved from https://doi.org/10.1002/met.1654

Wilks, D. S. (2011). *Statistical methods in the atmospheric sciences* (Vol. 100). Academic Press.

Xie, Y.-B., Chen, S.-J., Zhang, I.-L., & Hung, Y.-L. (1963). A preliminarily statistic and synoptic study about the basic currents over southeastern asia and the initiation of typhoon (in Chinese). *Acta Meteorological Sin.*, *33*, 206–217.

Ye, C., Deng, L., Huang, W.-R., & Chen, J. (2020). Comparison of the madden–julian oscillation-related tropical cyclone genesis over the south China sea and western north pacific under different el niño-southern oscillation conditions. *Atmosphere*, *11*(2), 183. Retrieved from https://doi.org/10.3390/atmos11020183

You, L., Gao, J., Lin, H., & Chen, S. (2019). Impact of the intra-seasonal oscillation on tropical cyclone genesis over the western north pacific. *International Journal of Climatology*, *39*(4), 1969–1984. Retrieved from https://doi.org/10.1002/joc.5927

Zhang, F., Sun, Y. Q., Magnusson, L., Buizza, R., Lin, S.-J., Chen, J.-H., & Emanuel, K. (2019). What is the predictability limit of midlatitude weather? *Journal of the Atmospheric Sciences*, *76*(4), 1077–1091. https://doi.org/10.1175/JAS-D-18-0269.1

Zhang, Q., Wu, L., & Liu, Q. (2009). Tropical cyclone damages in China 1983–2006. *Bulletin of the American Meteorological Society*, *90*(4), 489–496. Retrieved from https://doi.org/10.1175/2008BAMS2631.1

Zhang, Q., Zhang, W., Chen, Y., & Jiang, T. (2011). Flood, drought and typhoon disasters during the last half-century in the guangdong province, China. *Natural Hazards*, *57*(2), 267–278. https://doi.org/10.1007/s11069-010-9611-9

Zhao, H., Lu, Y., Jiang, X., Klotzbach, P. J., Wu, L., & Cao, J. (2022). A statistical intraseasonal prediction model of extended boreal summer western north pacific tropical cyclone genesis. *Journal of Climate*, *35*(8), 2459–2478. Retrieved from https://doi.org/10.1175/JCLI-D-21-0110.1